



## Article

# Enhanced Oral Bioavailability of Resveratrol by Using Neutralized Eudragit E Solid Dispersion Prepared via Spray Drying

Eun-Sol Ha <sup>1</sup>, Du Hyung Choi <sup>2</sup>, In-hwan Baek <sup>3</sup> , Heejun Park <sup>4</sup> and Min-Soo Kim <sup>1,\*</sup>

<sup>1</sup> College of Pharmacy, Pusan National University, 63 Busandaehak-ro, Geumjeong-gu, Busan 46241, Korea; edel@pusan.ac.kr

<sup>2</sup> Department of Pharmaceutical Engineering, Inje University, Gyeongsang 50834, Korea; choihd@inje.ac.kr

<sup>3</sup> College of Pharmacy, Kyungsung University, 309, Suyeong-ro, Nam-gu, Busan 48434, Korea; baek@ks.ac.kr

<sup>4</sup> College of Pharmacy, Duksung Women's University, 33, Samyangro 144-gil, Dobong-gu, Seoul 01369, Korea; heejunpark@duksung.ac.kr

\* Correspondence: minsookim@pusan.ac.kr; Tel.: +82-51-510-2813

**Abstract:** In this study, we designed amorphous solid dispersions based on Eudragit E/HCl (neutralized Eudragit E using hydrochloric acid) to maximize the dissolution of *trans*-resveratrol. Solid-state characterization of amorphous solid dispersions of *trans*-resveratrol was performed using powder X-ray diffraction, scanning electron microscopy, and particle size measurements. In addition, an in vitro dissolution study and an in vivo pharmacokinetic study in rats were carried out. Among the tested polymers, Eudragit E/HCl was the most effective solid dispersion for the solubilization of *trans*-resveratrol. Eudragit E/HCl significantly inhibited the precipitation of *trans*-resveratrol in a pH 1.2 dissolution medium in a dose-dependent manner. The amorphous Eudragit E/HCl solid dispersion at a *trans*-resveratrol/polymer ratio of 10/90 exhibited a high degree of supersaturation without *trans*-resveratrol precipitation for at least 48 h by the formation of Eudragit E/HCl micelles. In rats, the absolute oral bioavailability (F%) of *trans*-resveratrol from Eudragit E/HCl solid dispersion (10/90) was estimated to be 40%. Therefore, *trans*-resveratrol-loaded Eudragit E/HCl solid dispersions prepared by spray drying offer a promising formulation strategy with high oral bioavailability for developing high-quality health supplements, nutraceutical, and pharmaceutical products.

**Keywords:** bioavailability; solid dispersion; resveratrol; solubility



**Citation:** Ha, E.-S.; Choi, D.H.; Baek, I.-h.; Park, H.; Kim, M.-S. Enhanced Oral Bioavailability of Resveratrol by Using Neutralized Eudragit E Solid Dispersion Prepared via Spray Drying. *Antioxidants* **2021**, *10*, 90. <https://doi.org/10.3390/antiox10010090>

Received: 9 December 2020

Accepted: 9 January 2021

Published: 11 January 2021

**Publisher's Note:** MDPI stays neutral with regard to jurisdictional claims in published maps and institutional affiliations.



**Copyright:** © 2021 by the authors. Licensee MDPI, Basel, Switzerland. This article is an open access article distributed under the terms and conditions of the Creative Commons Attribution (CC BY) license (<https://creativecommons.org/licenses/by/4.0/>).

## 1. Introduction

*Trans*-resveratrol is an antioxidant phytochemical obtained from grapes, berries, and peanuts. The intake of *trans*-resveratrol from dietary supplements and red wine has been shown to have several therapeutic properties [1,2]. Most of the clinical trials involving resveratrol have focused on cancer (prostate, breast, and colorectal), neurological disorders (Alzheimer's disease and ischemic stroke), cardiovascular diseases (coronary artery disease, atherosclerosis, hypertension, and oxidative stress), diabetes (type 2 and impaired glucose tolerance), and non-alcoholic fatty liver disease [3]. Unfortunately, the use of *trans*-resveratrol by oral administration has been limited by its poor water solubility (below 60 µg/mL in the pH range of 1.2–6.8), instability (conversion of *trans*-resveratrol to *cis*-resveratrol, chemical degradation by alkalizers, and ultraviolet light), and rapid metabolism in the liver, impeding the efficacy of its therapeutic benefits [4–7]. In an attempt to improve the oral bioavailability of *trans*-resveratrol, several different strategies such as cyclodextrin complexes, cocrystals, liposomes, composite nanoparticles, solid dispersions, solid lipid nanoparticles, microemulsions, self-microemulsifying drug delivery systems, polymeric micelles, nanosuspensions, and nanocrystals have been used [8–18]. Most of these previous attempts have added a large amount of surfactant to the formulation. The absorption is typically higher for the formulations that use a lot of surfactants

compared with that of the raw drug material [17,18], but the higher risk of side effects could be resulted in when taken for a long period of time. Thus, it is necessary to develop a formulation that uses less surfactant. We recently developed composite nanoparticles and pure *trans*-resveratrol nanoparticles with high bioavailability using a supercritical anti-solvent (SAS) process [19,20]. Furthermore, we demonstrated that the oral bioavailability of *trans*-resveratrol can be increased by improving the dissolution rate and supersaturation of *trans*-resveratrol in an in vitro dissolution test. Regrettably, the mass production of nanoparticles using the SAS process is difficult due to the high cost of high-pressure equipment at a commercial scale of production [21].

In the present study, we hypothesize that an increase in supersaturation of a *trans*-resveratrol solution based on amorphous solid dispersions translates to higher oral bioavailability. Therefore, we designed amorphous solid dispersions using Eudragit E/HCl (Eudragit E neutralized using hydrochloric acid) to maximize the dissolution of *trans*-resveratrol. Eudragit E, a cationic copolymer based on methacrylate, dissolves under conditions with pH < 5.0, while neutralized Eudragit E can be dissolved under intestinal conditions (pH 6.8–8.0) as well as acidic conditions [22–24]. Spray drying, commonly used in the preparation of numerous commercialized products, was used to produce amorphous solid dispersions [25–28]. Besides Eudragit E/HCl, other amorphous solid dispersions of *trans*-resveratrol were produced using different hydrophilic polymers for comparison purposes. Solid-state characterization of amorphous solid dispersions of *trans*-resveratrol was performed using powder X-ray diffraction (PXRD), scanning electron microscopy (SEM), and particle size measurements. Furthermore, an in vitro dissolution test in non-sink conditions and an in vivo oral bioavailability study in rats were carried out to compare different solid dispersions manufactured using the spray drying process.

## 2. Materials and Methods

### 2.1. Materials

*Trans*-resveratrol was provided by Ningbo Liwah Pharmaceutical Co., Ltd. (Ningbo, China). Eudragit E PO (powder form of a cationic copolymer based on dimethylaminoethyl methacrylate, butyl methacrylate, and methyl methacrylate with a ratio of 2:1:1), polyvinylpyrrolidone K30 (PVP K30), and polyvinylpyrrolidone vinyl acetate 64 (PVP VA 64) were kindly donated by BASF (Ludwigshafen, Germany). Hydroxypropylmethyl cellulose (HPMC 6 cp) and hydroxypropyl cellulose (HPC-L) were kindly donated by Shin-Etsu Chemical Co., Ltd. (Tokyo, Japan), and Nippon Soda Co., Ltd. (Tokyo, Japan), respectively. Eudragit E/HCl (neutralized Eudragit E with hydrochloric acid) powder was prepared as previously reported [29]. All organic solvents of high-performance liquid chromatography (HPLC) grade were purchased from J.T. Baker (Phillipsburg, NJ, USA). All reagents used were of analytical grade and purchased from Sigma-Aldrich Co., Ltd. (St Louis, MO, USA) or Daejung Chemicals and Metals Co., Ltd. (Siheung-si, Korea).

### 2.2. Preparation of *Trans*-Resveratrol Solid Dispersion Using the Spray Drying Process

*Trans*-resveratrol solid dispersions with different polymers at various ratios were produced using a B-191 laboratory-scale spray dryer (Buchi, Flawil, Switzerland). The polymers (Eudragit E/HCl, HPC-L, PVP K30, and PVP VA64) and *trans*-resveratrol were dissolved in ethanol at a concentration of 3% *w/v* while HPMC was dissolved in a 70% ethanol solution. The solutions were delivered into the inner line of a two-fluid nozzle at a constant flow rate of 4–6 mL/min using a peristaltic pump. The nozzle's outer line was supplied with atomization air pressure regulated to 5 kPa, and the solution and drying air were in the same flow direction. Spray drying was carried out in a drying room with an inlet temperature of 80–100 °C and an outlet temperature of 55–70 °C. The prepared powder was obtained in a particle collection chamber equipped with a cyclone.

### 2.3. Morphology Observation and Particle Size Measurement

The morphology of solid dispersion particles was observed using a HITACHI S3500N scanning electron microscope (SEM, Tokyo, Japan). The sample was placed on a brass stub with double-sided electrically conductive adhesive tape and coated with platinum for 60 s under vacuum using an ion sputter to provide electrical conductivity. The image was acquired at a beam acceleration voltage of 30 kV and 1500 times magnification. The particle size and distribution of the spray-dried samples were determined using a HELOS laser diffraction analyzer (Sympatec GmbH, Clausthal-Zellerfeld, Germany). The powder dispersion was made uniform using a RODOS vibrating trough disperser at an air pressure of 0.1 MPa and 5.3 kPa vacuum conditions.

### 2.4. HPLC Analysis

The *trans*-resveratrol content incorporated with the solid dispersion particles was calculated by HPLC analysis of sample solutions prepared by dissolving the solid dispersion particles in ethanol or a 70% ethanol solution. HPLC analysis was conducted using an Agilent 1260 Infinity HPLC system (Agilent Technologies, Santa Clara, CA, USA). A Gemini C18 reversed-phase column (Phenomenex, 150 × 4.6 mm, 5 μm) was used for chromatographic separation using a 40% acetonitrile solution as the mobile phase at a constant flow rate of 0.8 mL/min at 30 °C. Samples of 10 μL were injected and detected at a wavelength of 303 nm.

### 2.5. Powder X-ray Diffraction (PXRD)

The conversion to amorphous solid dispersions was assessed by recording the PXRD patterns of the solid dispersion particles using an Xpert 3 X-ray diffractometer (PHILIPS, Almelo, The Netherlands) at a 1°/min scan rate in the 2θ range of 5–50°.

### 2.6. Dissolution Test

To assess the enhanced dissolution property of *trans*-resveratrol, solid dispersion particles equivalent to 200 mg of *trans*-resveratrol were placed into 500 mL of a pH 1.2 or pH 6.8 dissolution medium at 37 ± 0.5 °C, with a paddle rotation of 100 rpm using a dissolution system (Model 708-DS, Agilent Technologies, Santa Clara, CA, USA). At 0.083, 0.167, 0.25, 0.5, 1, 2, 3, 4, 6, and 24 h post-dissolution test, 3 mL samples were drawn from the vessels and passed through 0.22 μm syringe filters. HPLC analysis was conducted following dilution of the filtered samples with methanol. All sample tests were repeated four times (Tables S1–S4, Supplementary Materials).

### 2.7. Dynamic Light Scattering Measurement

Dynamic light scattering (DLS) measurements were conducted using an ELSZ-1000 particle analyzer (Otsuka Electronics, Tokyo, Japan), according to the manufacturer's instructions (a scattering angle of 165°), to evaluate the particle size of the sample solutions obtained from the dissolution test. Each sample was measured in triplicate using a He-Ne laser light source (666 nm).

### 2.8. Bioavailability Study in Rats

To evaluate the oral bioavailability of *trans*-resveratrol solid dispersion particles, the in vivo pharmacokinetics of *trans*-resveratrol were investigated using male Sprague-Dawley (SD) rats (200 ± 10 g; Hyochang Science, Daegu, Korea). The animal study protocol complied with the institutional guidelines for the care and use of laboratory animals and was approved by the ethics committee of Kyungsung University (No. 20-017A). Four groups of the rats (five rats per group) were each orally administered via gastric gavage any one of the *trans*-resveratrol raw material, HPMC solid dispersion (10/90), Eudragit E solid dispersion (25/75), and Eudragit E/HCl solid dispersion (10/90) at a dose of 20 mg/kg as *trans*-resveratrol via dispersion state in 1 mL of water before dosing. Blood samples were collected from the jugular vein into heparinized tubes at predetermined time points

of prior administration (0 h), 0.25, 0.5, 0.75, 1, 1.5, 2, 4, 6, and 8 h after oral administration. The plasma was separated from the blood samples immediately by centrifugation for 10 min at  $6010\times g$ . HPLC analysis was used to determine the plasma concentrations of *trans*-resveratrol as previously described [30]. The area under the plasma concentration-time curve ( $AUC_{0\rightarrow 8h}$ ) was estimated based on the linear trapezoidal rule. The maximum *trans*-resveratrol concentration in plasma ( $C_{max}$ ) and the time to reach  $C_{max}$  ( $T_{max}$ ) were determined directly from the individual datum.

### 2.9. Statistical Analysis

The differences among the groups were determined using one-way analysis of variance (ANOVA), and post hoc mean separation was conducted using the least-squares difference (LSD) or Student-Newman-Keuls (SNK) tests. Analyses were performed using SPSS 25.0 software (IBM SPSS Statistics, IBM Corporation, Armonk, NY, USA).

## 3. Results and Discussion

*Trans*-resveratrol solid dispersion powders with Eudragit E/HCl, HPMC, HPC, PVP, or PVP VA64 were prepared via spray drying. *Trans*-resveratrol was successfully dispersed into the solid dispersion powders as the encapsulation efficiency was above 96% in all formulations (Table 1). Furthermore, the process yield was above 75% for all formulations. As shown in Figure 1, the raw morphology is needle-shaped, with a mean particle size of 52.5  $\mu\text{m}$ , and the solid dispersion powders were observed as irregularly shaped microparticles. Samples of raw *trans*-resveratrol and solid dispersion powders were analyzed using PXRD to assess the production of amorphous solid dispersions of *trans*-resveratrol (Figure 2). Raw *trans*-resveratrol showed characteristic peaks at 2 $\theta$ , similar to previously reported data [16]. However, the characteristic crystalline peaks of *trans*-resveratrol were not detected for all solid dispersion powders prepared, indicating amorphous *trans*-resveratrol in the solid dispersions.

**Table 1.** Encapsulation efficiency and particle size of raw *trans*-resveratrol and solid dispersion powders produced using the spray drying process.

Solid Dispersions ( <i>Trans</i> -Resveratrol/Polymer Ratio)	Encapsulation Efficiency <sup>a</sup> (%)	Volume Mean Particle Size <sup>a</sup> ( $\mu\text{m}$ )
HPC (25/75)	97.7 $\pm$ 1.5	4.84 $\pm$ 0.31 (1.89) <sup>b</sup>
HPC (10/90)	96.9 $\pm$ 2.1	4.12 $\pm$ 0.23 (1.83)
HPMC (25/75)	98.9 $\pm$ 1.4	5.23 $\pm$ 0.31 (1.93)
HPMC (10/90)	98.3 $\pm$ 1.1	4.98 $\pm$ 0.22 (1.81)
PVP K30 (25/75)	99.1 $\pm$ 1.0	4.03 $\pm$ 0.21 (1.71)
PVP K30 (10/90)	98.2 $\pm$ 0.9	3.98 $\pm$ 0.19 (1.65)
PVP VA64 (25/75)	98.6 $\pm$ 1.2	3.69 $\pm$ 0.32 (1.65)
PVP VA64 (10/90)	98.8 $\pm$ 1.1	3.98 $\pm$ 0.19 (1.69)
Eudragit E/HCl (25/75)	98.2 $\pm$ 0.8	3.76 $\pm$ 0.29 (1.53)
Eudragit E/HCl (10/90)	98.0 $\pm$ 0.5	3.92 $\pm$ 0.27 (1.62)
Eudragit E/HCl (20/80)	98.3 $\pm$ 0.9	3.89 $\pm$ 0.15 (1.71)
Eudragit E/HCl (15/85)	98.6 $\pm$ 0.6	4.01 $\pm$ 0.32 (1.65)
Raw <i>trans</i> -resveratrol	-	52.5 $\pm$ 1.32 (2.21)

<sup>a</sup> Mean  $\pm$  standard deviation ( $n = 4$ ). <sup>b</sup> The span is the width of the distribution and is calculated as follows  $(d_{90} - d_{10})/d_{50}$ , where  $d_{10}$ ,  $d_{50}$ , and  $d_{90}$  are the diameter sizes at 10%, 50%, and 90% in a cumulative size distribution, respectively.



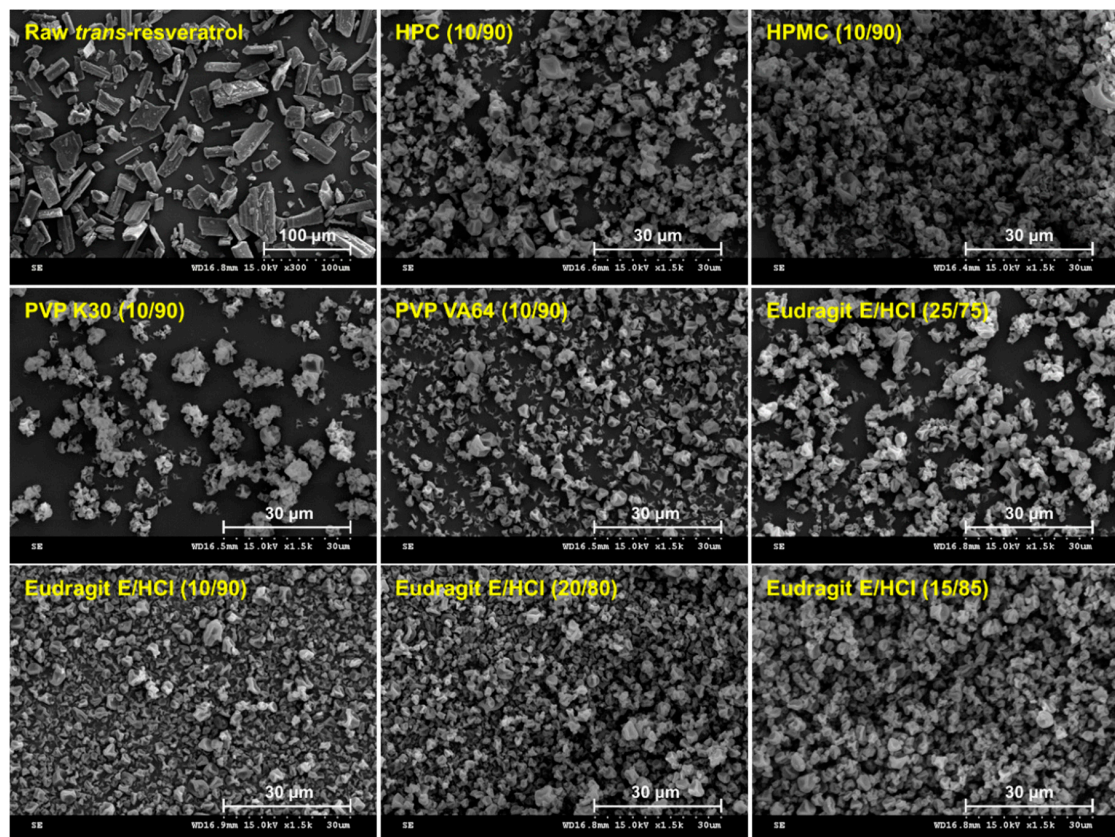


**Figure 1.** Scanning electron microscope images of raw *trans*-resveratrol and solid dispersion powders produced using the spray drying process.

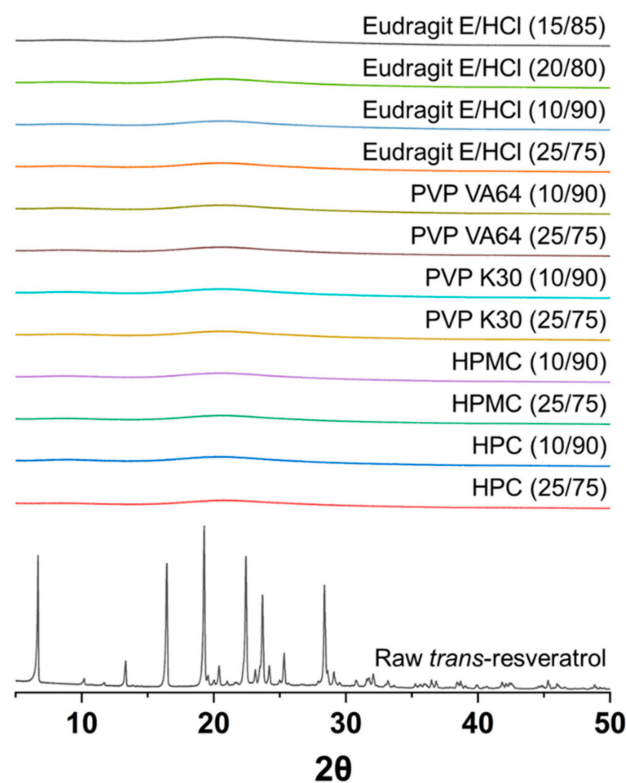


**Figure 2.** Powder X-ray diffraction patterns of raw *trans*-resveratrol and solid dispersion powders produced using the spray drying process.

### 3.1. Dissolution Data

The enhanced dissolution properties of *trans*-resveratrol by amorphous solid dispersions were investigated using dissolution studies in pH 1.2 or pH 6.8 dissolution medium (non-sink condition). As shown in Figure 3, raw *trans*-resveratrol exhibited a slow rate and low degree of dissolution in pH 1.2 and 6.8 dissolution media because of its low solubility at pH 1.2 (52.3 µg/mL) and pH 6.8 (51.1 µg/mL) at 37 °C [19]. At a *trans*-resveratrol/polymer ratio of 25/75, Eudragit E/HCl showed a rapid dissolution rate, a maximum concentration of 365 µg/mL, and gradual subsequent precipitation of *trans*-resveratrol in the pH 1.2 dissolution medium. The concentration of *trans*-resveratrol at 120 min ranked by the SNK test increased in the following order: Eudragit E/HCl solid dispersion > HPMC solid dispersion > HPC solid dispersion > PVP solid dispersion, and PVP VA solid dispersion > raw *trans*-resveratrol. The dissolution data at pH 6.8 showed a similar trend to that at pH 1.2. Generally, the supersaturation and dissolution of poorly water-soluble compounds were enhanced by increasing the hydrophilic polymer amount in the amorphous solid dispersions [31–35]. As shown in Figure 3, dissolution of *trans*-resveratrol was not significantly improved at a *trans*-resveratrol/polymer ratio of 10/90 compared with the other polymers, except Eudragit E/HCl. However, *trans*-resveratrol from the Eudragit E/HCl solid dispersion at a 10/90 ratio was completely dissolved within 30 min in pH 1.2 and pH 6.8 dissolution media. In addition, the precipitation of *trans*-resveratrol did not occur until at least 2 h in pH 1.2 and 6 h in pH 6.8 dissolution media. Among the tested polymers, Eudragit E/HCl was the most effective solid dispersion for the solubilization of *trans*-resveratrol.

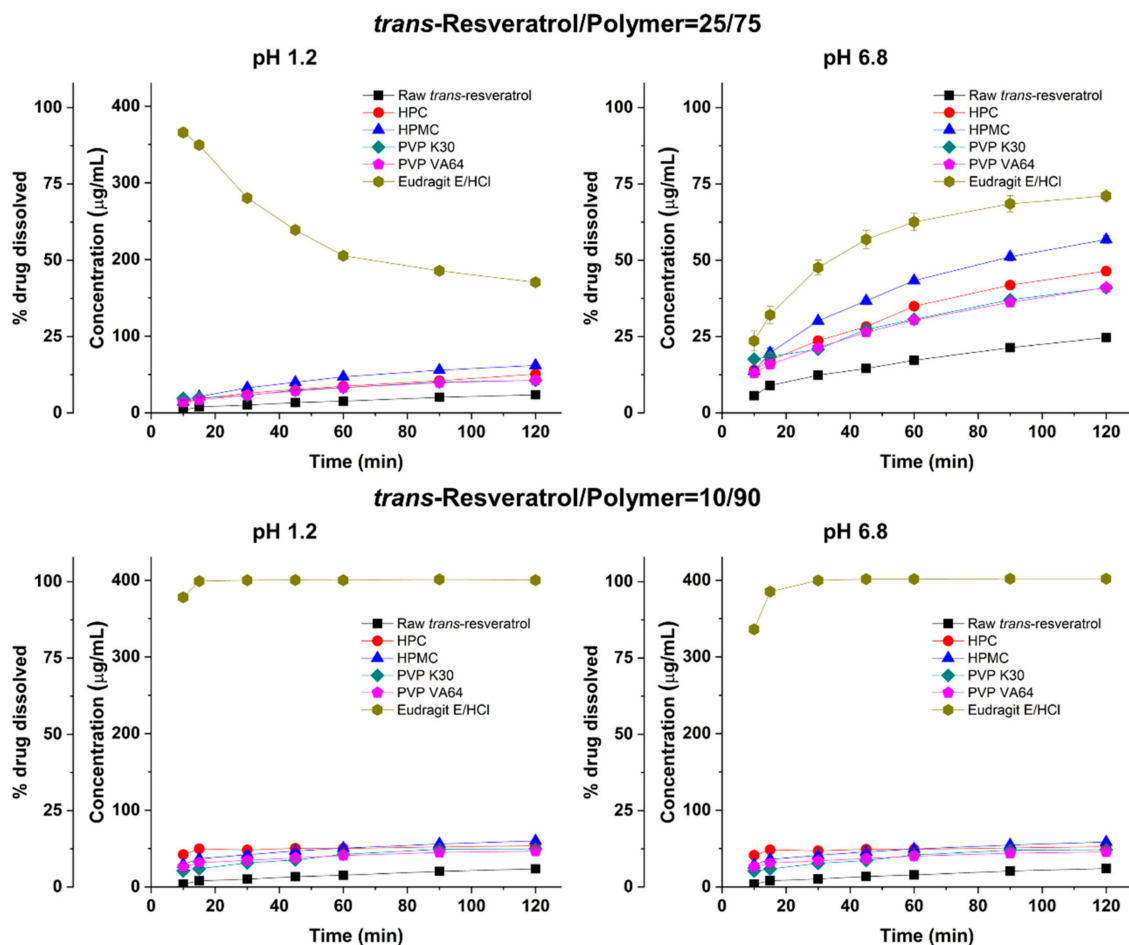


**Figure 3.** Dissolution profiles of raw *trans*-resveratrol and solid dispersion powders produced using the spray drying process in pH 1.2 and 6.8 dissolution media.

Generally, the supersaturated state acquired through amorphous solid dispersion in the dissolution medium is thermodynamically unstable, and subsequent return to the thermodynamically stable state occurs via precipitation [36–39]. The degree of supersaturation and inhibition of the precipitation of poorly water-soluble compounds can be controlled by using a hydrophilic polymer [40,41]. The polymer acts as a precipitation inhibitor that inhibits crystal growth by blocking the active surface or forming specific interactions with poorly water-soluble compounds. Previously, Wegiel and co-workers reported on the specific interactions between *trans*-resveratrol and polymers by performing spectroscopic analysis [42]. They observed that the increasing order of strength of the hydrogen bonds (the OH stretching region: 3350–2750  $\text{cm}^{-1}$ ) was in the order: PVP > HPMC > Eudragit E, while the ionic interactions related to *trans*-resveratrol crystallization inhibiting performance increased as follows: Eudragit E > PVP > HPMC. Thus, it was suggested that the high degree of supersaturation with an extended supersaturation observed with Eudragit E/HCl might be due to the hydrogen bonding and ionic interactions between *trans*-resveratrol and Eudragit E.

To further investigate the effect of Eudragit E/HCl on the dissolution of *trans*-resveratrol, amorphous solid dispersions were prepared at different *trans*-resveratrol/Eudragit E/HCl ratios of 25/75, 20/80, 15/85, and 10/90 and evaluated for 48 h in a pH 1.2 or pH 6.8 dissolution medium (non-sink condition). As shown in Figure 4, a high degree of supersaturation was observed within 30 min at all ratios, and Eudragit E/HCl significantly inhibited the precipitation of *trans*-resveratrol in the pH 1.2 dissolution medium in a dose-dependent manner. However, the degree of supersaturation of *trans*-resveratrol was enhanced by Eudragit E/HCl in the pH 6.8 dissolution medium in a dose-dependent manner. Interestingly, *trans*-resveratrol from the Eudragit E/HCl solid dispersion at a 10/90 ratio was completely dissolved within 30 min, and precipitation did not occur until at least 48 h in both the pH 1.2 and pH 6.8 dissolution media. At this time, DLS measurements were carried out to evaluate the soluble state of *trans*-resveratrol. As depicted in Figure 4, the solution's mean particle size was 10.9 nm for pH 1.2 and 53.6 nm for pH 6.8. Yoshida and co-workers demonstrated micelle formation at Eudragit E/HCl concentrations above 30  $\mu\text{g}/\text{mL}$ , and the particle size of tacrolimus-loaded Eudragit E/HCl micelles varied from 10 to 369.8 nm in different medium conditions [22,24]. Recently, Lin and co-workers reported the solubilization of ibuprofen, felodipine, and bifendate by Eudragit E in HCl solution via micelle formation [43]. In fact, the high solubilization of *trans*-resveratrol by Eudragit E/HCl solid dispersion prepared by the spray drying process might be used to estimate the formation of Eudragit E/HCl micelles, similar to previously reported poorly water-soluble compounds.

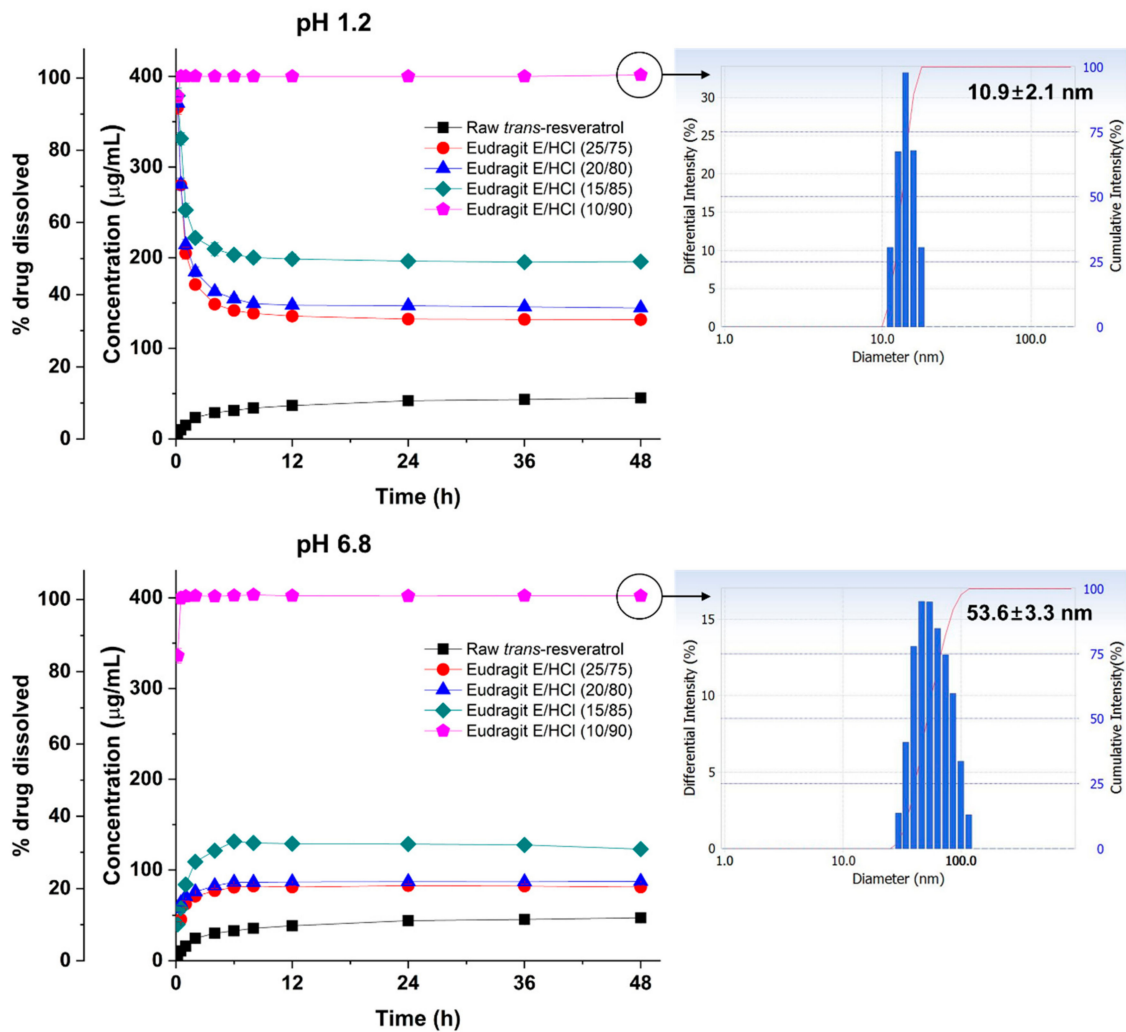


**Figure 4.** Effect of Eudragit E/HCl ratio on the dissolution of *trans*-resveratrol from solid dispersions in pH 1.2 and 6.8 dissolution media.

### 3.2. Oral Bioavailability in SD Rats

The effects of the observed degree and duration of *in vitro* supersaturation on *trans*-resveratrol bioavailability were further investigated by the determination of *in vivo* pharmacokinetic parameters using oral administration of raw *trans*-resveratrol, HPMC solid dispersion (10/90), and Eudragit E/HCl solid dispersion at 25/75 and 10/90 ratios to SD rats (Table 2). Furthermore, the absolute oral bioavailability ( $F\%$ ) of *trans*-resveratrol was estimated by dividing the  $AUC_{0 \rightarrow 8\text{ h}}$  value obtained from oral administration by the  $AUC_{0 \rightarrow 8\text{ h}}$  value obtained from intravenous administration with dose normalization. The  $AUC_{0 \rightarrow 8\text{ h}}$  value of *trans*-resveratrol after intravenous administration used was from our previous study [20]. As shown in Figure 5, the oral absorption of *trans*-resveratrol was significantly enhanced by the Eudragit E/HCl solid dispersion. In addition, the Eudragit E/HCl solid dispersion (10/90) was 4.2- and 5.5-fold higher in  $AUC_{0 \rightarrow 8\text{ h}}$  and  $C_{\text{max}}$  values respectively, than raw *trans*-resveratrol. Based on the ANOVA, there were significant differences among the solid dispersions ( $p < 0.05$ ), which, in order of increasing pharmacokinetic parameters, were ranked by the SNK test as follows: raw *trans*-resveratrol < HPMC solid dispersion (10/90) = Eudragit E/HCl solid dispersion (25/75) < Eudragit E/HCl solid dispersion (10/90) for  $AUC_{0 \rightarrow 8\text{ h}}$  values, and raw *trans*-resveratrol < HPMC solid dispersion (10/90) < Eudragit E/HCl solid dispersion (25/75) < Eudragit E/HCl solid dispersion (10/90) for  $C_{\text{max}}$  values. In fact, the  $AUC_{0 \rightarrow 8\text{ h}}$  and  $C_{\text{max}}$  values of *trans*-resveratrol increased with the increasing degree and duration of *in vitro* supersaturation. This ten-



gency is similar to that of *trans*-resveratrol-loaded composite nanoparticles previously reported [20,21]. Furthermore, the absolute oral bioavailability (F%) of *trans*-resveratrol was estimated to be 40% for the Eudragit E/HCl solid dispersion (10/90). Previously, it was revealed that the absolute oral bioavailability (F%) of *trans*-resveratrol in rats varied between 2.6% and 46.4% in different solubilizing formulation systems [44–47]. Thus, Eudragit E/HCl solid dispersion prepared by spray drying is an effective oral formulation with high absolute bioavailability for poorly water-soluble *trans*-resveratrol.

**Table 2.** Pharmacokinetic parameters of *trans*-resveratrol in rats after oral administration of raw *trans*-resveratrol or solid dispersions.

Solid Dispersions ( <i>Trans</i> -Resveratrol/Polymer Ratio)	AUC <sub>0→8h</sub> (ng·h/mL)	C <sub>max</sub> (ng/mL)	T <sub>max</sub> (h)	F (%)
Eudragit E/HCl (25/75)	330.0 ± 41.8 <sup>a</sup>	109.6 ± 22.4 <sup>a,b</sup>	1.0 ± 0.3	22.6
Eudragit E/HCl (10/90)	583.9 ± 92.1 <sup>a,b,c</sup>	204.4 ± 25.5 <sup>a,b,c</sup>	0.8 ± 0.2	40.0
HPMC (10/90)	279.8 ± 40.7 <sup>a</sup>	79.6 ± 11.2 <sup>a</sup>	1.1 ± 0.4	19.2
Raw <i>trans</i> -resveratrol	138.9 ± 22.0	37.0 ± 7.7	1.2 ± 0.3	9.5

Note: <sup>a</sup>  $p < 0.05$  vs. raw *trans*-resveratrol; <sup>b</sup>  $p < 0.05$  vs. HPMC solid dispersion (10/90) <sup>c</sup>  $p < 0.05$  vs. Eudragit E/HCl solid dispersion (25/75). Mean ± standard deviation ( $n = 5$ ). AUC<sub>0→8h</sub>, the area under the plasma concentration versus time curve; C<sub>max</sub>, the maximum plasma concentration of *trans*-resveratrol; T<sub>max</sub>, the time required to reach C<sub>max</sub>; F (%), the absolute oral bioavailability.

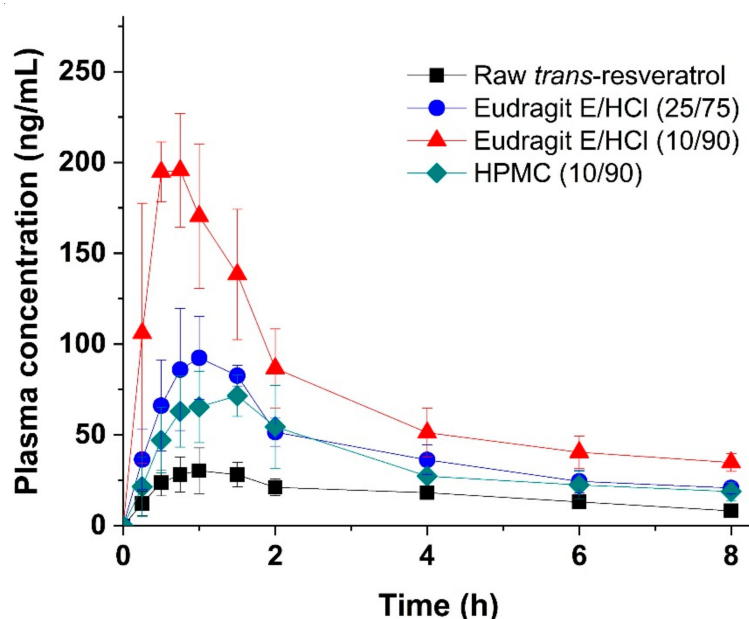


**Figure 5.** Plasma concentration-time profiles of raw *trans*-resveratrol and solid dispersion powders produced using the spray drying process after oral administration in Sprague-Dawley rats.

#### 4. Conclusions

In the present study, we presented an amorphous solid dispersion of *trans*-resveratrol through a Eudragit E/HCl solid dispersion prepared by a spray drying process. The amorphous Eudragit E/HCl solid dispersion at a *trans*-resveratrol/polymer ratio of 10/90 exhibited a high degree of supersaturation without precipitation of *trans*-resveratrol for at least 48 h by the formation of Eudragit E/HCl micelles. In SD rats, the absolute oral bioavailability (F%) of *trans*-resveratrol from the Eudragit E/HCl solid dispersion (10/90) was estimated to be 40%. Therefore, *trans*-resveratrol-loaded Eudragit E/HCl solid dispersions prepared by spray drying offer a promising formulation strategy with high oral bioavailability for developing high-quality health supplements, nutraceutical, and pharmaceutical products.

**Supplementary Materials:** The following are available online at <https://www.mdpi.com/2076-3921/10/1/90/s1>, Table S1: Dissolution data (concentration, µg/mL) of raw trans-resveratrol and solid dispersion powders produced using the spray drying process in pH 1.2 dissolution media, Table S2: Dissolution data (concentration, µg/mL) of raw trans-resveratrol and solid dispersion powders produced using the spray drying process in pH 6.8 dissolution media, Table S3: Dissolution data (concentration, µg/mL) of raw trans-resveratrol and Eudragit E/HCl solid dispersion powders produced using the spray drying process in pH 1.2 dissolution media, Table S4: Dissolution data (concentration, µg/mL) of raw trans-resveratrol and Eudragit E/HCl solid dispersion powders produced using the spray drying process in pH 6.8 dissolution media.

**Author Contributions:** Conceptualization, E.-S.H., D.H.C. and M.-S.K.; formal analysis, E.-S.H., I.-h.B. and M.-S.K.; funding acquisition, M.-S.K.; investigation, E.-S.H., D.H.C. and M.-S.K.; methodology, E.-S.H., I.-h.B., H.P. and M.-S.K.; software, E.-S.H., I.-h.B. and M.-S.K.; supervision, M.-S.K.; validation, E.-S.H.; writing—original draft, E.-S.H.; writing—review and editing, E.-S.H., D.H.C., I.-h.B., H.P. and M.-S.K. All authors have read and agreed to the published version of the manuscript.

**Funding:** This study was financially supported by the 2020 Post-Doc. Development Program of Pusan National University. This work was supported by the National Research Foundation of Korea (NRF) grant funded by the Korea government (MSIT) (No. 2020R1A2C4002166).

**Institutional Review Board Statement:** The animal study protocol complied with the institutional guidelines for the care and use of laboratory animals and was approved by the ethics committee of Kyungsoong University (protocol code: No. 20-017A and date of approval: 21 July 2020).

**Informed Consent Statement:** Not applicable.

**Data Availability Statement:** The data presented in this study are available on request from the corresponding author.

**Conflicts of Interest:** The authors declare no conflict of interest.

## References

1. Esparza, I.; Cimminelli, M.J.; Moler, J.A.; Jiménez-Moreno, N.; Ancín-Azpilicueta, C. Stability of Phenolic Compounds in Grape Stem Extracts. *Antioxidants* **2020**, *9*, 720. [[CrossRef](#)]
2. Rodríguez-Varela, C.; Labarta, E. Clinical Application of Antioxidants to Improve Human Oocyte Mitochondrial Function: A Review. *Antioxidants* **2020**, *9*, 1197. [[CrossRef](#)]
3. Berman, A.Y.; Motechin, R.A.; Wiesenfeld, M.Y.; Holz, M.K. The therapeutic potential of resveratrol: A review of clinical trials. *NPJ Precis. Oncol.* **2017**, *1*, 35. [[CrossRef](#)] [[PubMed](#)]
4. Amri, A.; Chaumeil, J.C.; Sfar, S.; Charrueau, C. Administration of resveratrol: What formulation solutions to bioavailability limitations? *J. Control. Release* **2012**, *158*, 182–193. [[CrossRef](#)] [[PubMed](#)]
5. Zhao, Y.; Shi, M.; Ye, J.-H.; Zheng, X.-Q.; Lu, J.-L.; Liang, Y.-R. Photo-induced chemical reaction of trans-resveratrol. *Food Chem.* **2015**, *171*, 137–143. [[CrossRef](#)] [[PubMed](#)]
6. Marier, J.F.; Vachon, P.; Gritsas, A.; Zhang, J.; Moreau, J.P.; Ducharme, M.P. Metabolism and disposition of resveratrol in rats: Extent of absorption, glucuronidation, and enterohepatic recirculation evidenced by a linked-rat model. *J. Pharmacol. Exp. Ther.* **2002**, *302*, 369–373. [[CrossRef](#)] [[PubMed](#)]
7. Walle, T. Bioavailability of resveratrol. *Ann. N. Y. Acad. Sci.* **2011**, *1215*, 9–15. [[CrossRef](#)] [[PubMed](#)]
8. Mamadou, G.; Charrueau, C.; Dairou, J.; Nzouzi, N.L.; Eto, B.; Ponchel, G. Increased intestinal permeation and modulation of presystemic metabolism of resveratrol formulated into self-emulsifying drug delivery systems. *Int. J. Pharm.* **2017**, *521*, 150–155. [[CrossRef](#)] [[PubMed](#)]
9. Intagliata, S.; Modica, M.N.; Santagati, L.M.; Montenegro, L. Strategies to improve resveratrol systemic and topical bioavailability: An update. *Antioxidants* **2019**, *8*, 244. [[CrossRef](#)] [[PubMed](#)]
10. Aguiar, G.P.S.; Boschetto, D.L.; Chaves, L.M.P.C.; Arcari, B.D.; Piato, A.L.; Oliveira, J.V.; Lanza, M. Trans-resveratrol micronization by SEDS technique. *Ind. Crops Prod.* **2016**, *89*, 350–355. [[CrossRef](#)]
11. Zu, Y.; Zhang, Y.; Wang, W.; Zhao, X.; Han, X.; Wang, K.; Ge, Y. Preparation and in vitro/in vivo evaluation of resveratrol-loaded carboxymethyl chitosan nanoparticles. *Drug Deliv.* **2016**, *23*, 981–991. [[CrossRef](#)] [[PubMed](#)]
12. Dhakar, N.K.; Matencio, A.; Caldera, F.; Argenziano, M.; Cavalli, R.; Dianzani, C.; Zanetti, M.; López-Nicolás, J.M.; Trotta, F. Comparative evaluation of solubility, cytotoxicity and photostability studies of resveratrol and oxyresveratrol loaded nanosponges. *Pharmaceutics* **2019**, *11*, 545. [[CrossRef](#)] [[PubMed](#)]
13. Kuk, D.-H.; Ha, E.-S.; Ha, D.-H.; Sim, W.-Y.; Lee, S.-K.; Jeong, J.-S.; Kim, J.-S.; Baek, I.-H.; Park, H.; Choi, D.H.; et al. Development of a resveratrol nanosuspension using the antisolvent precipitation method without solvent removal, based on a quality by design (QbD) approach. *Pharmaceutics* **2019**, *11*, 688. [[CrossRef](#)] [[PubMed](#)]

14. He, H.; Zhang, Q.; Wang, J.-R.; Mei, X. Structure, physicochemical properties and pharmacokinetics of resveratrol and piperine cocrystals. *Cryst. Eng. Comm.* **2017**, *19*, 6154–6163. [[CrossRef](#)]
15. Shimojo, A.A.M.; Fernandes, A.R.V.; Ferreira, N.R.E.; Sanchez-Lopez, E.; Santana, M.H.A.; Souto, E.B. Evaluation of the influence of process parameters on the properties of resveratrol-loaded NLC using 2<sup>2</sup> full factorial design. *Antioxidants* **2019**, *8*, 272. [[CrossRef](#)] [[PubMed](#)]
16. Aguiar, G.P.S.; Arcari, B.D.; Chaves, L.M.P.C.; Magro, C.D.; Boschetto, D.L.; Piato, A.L.; Lanza, M.; Oliveira, J.V. Micronization of trans-resveratrol by supercritical fluid: Dissolution, solubility and in vitro antioxidant activity. *Ind. Crops Prod.* **2018**, *112*, 1–5. [[CrossRef](#)]
17. Amiot, M.J.; Romier, B.; Dao, T.M.; Fanciullino, R.; Ciccolini, J.; Burcelin, R.; Pechere, L.; Emond, C.; Savouret, J.F.; Seree, E. Optimization of trans-resveratrol bioavailability for human therapy. *Biochimie* **2013**, *95*, 1233–1238. [[CrossRef](#)]
18. Calvo-Castro, L.A.; Schiborr, C.; David, F.; Ehrh, H.; Voggel, J.; Sus, N.; Behnam, D.; Bosy-Westphal, A.; Frank, J. The oral bioavailability of trans-resveratrol from a grapevine-shoot extract in healthy humans is significantly increased by micellar solubilization. *Mol. Nutr. Food Res.* **2018**, *62*, 1701057. [[CrossRef](#)]
19. Ha, E.-S.; Sim, W.-Y.; Lee, S.-K.; Jeong, J.-S.; Kim, J.-S.; Baek, I.-H.; Choi, D.H.; Park, H.; Hwang, S.-J.; Kim, M.-S. Preparation and evaluation of resveratrol-loaded composite nanoparticles using a supercritical fluid technology for enhanced oral and skin delivery. *Antioxidants* **2019**, *8*, 554. [[CrossRef](#)]
20. Ha, E.-S.; Park, H.; Lee, S.-K.; Sim, W.-Y.; Jeong, J.-S.; Baek, I.-H.; Kim, M.-S. Pure Trans-Resveratrol Nanoparticles Prepared by a Supercritical Antisolvent Process Using Alcohol and Dichloromethane Mixtures: Effect of Particle Size on Dissolution and Bioavailability in Rats. *Antioxidants* **2020**, *9*, 342. [[CrossRef](#)]
21. Cho, W.; Kim, M.-S.; Jung, M.-S.; Park, J.; Cha, K.-H.; Kim, J.-S.; Park, H.J.; Alhalaweh, A.; Velaga, S.P.; Hwang, S.-J. Design of salmon calcitonin particles for nasal delivery using spray-drying and novel supercritical fluid-assisted spray-drying processes. *Int. J. Pharm.* **2015**, *478*, 288–296. [[CrossRef](#)] [[PubMed](#)]
22. Yoshida, T.; Kurimoto, I.; Yoshihara, K.; Umejima, H.; Ito, N.; Watanabe, S.; Sako, K.; Kikuchi, A. Aminoalkyl methacrylate copolymers for improving the solubility of tacrolimus. I: Evaluation of solid dispersion formulations. *Int. J. Pharm.* **2012**, *428*, 18–24. [[CrossRef](#)] [[PubMed](#)]
23. Yoshida, T.; Kurimoto, I.; Yoshihara, K.; Umejima, H.; Ito, N.; Watanabe, S.; Sako, K.; Kikuchi, A. Effect of aminoalkyl methacrylate copolymer E/ HCl on in vivo absorption of poorly water-soluble drug. *Drug Dev. Ind. Pharm.* **2013**, *39*, 1698–1705. [[CrossRef](#)] [[PubMed](#)]
24. Yoshida, T.; Kurimoto, I.; Yoshihara, K.; Umejima, H.; Ito, N.; Watanabe, S.; Sako, K.; Kikuchi, A. Effects of dissolved state of aminoalkyl methacrylate copolymer E/HCl on solubility enhancement effect for poorly water-soluble drugs. *Colloid Polym. Sci.* **2013**, *291*, 1191–1199. [[CrossRef](#)]
25. Arpagaus, C. PLA/PLGA nanoparticles prepared by nano spray drying. *J. Pharm. Investig.* **2019**, *49*, 405–426. [[CrossRef](#)]
26. Maniyar, M.G.; Kokare, C.R. Formulation and evaluation of spray dried liposomes of lopinavir for topical application. *J. Pharm. Investig.* **2019**, *49*, 259–270. [[CrossRef](#)]
27. Ha, E.-S.; Baek, I.; Cho, W.; Hwang, S.-J.; Kim, M.-S. Preparation and Evaluation of Solid Dispersion of Atorvastatin Calcium with Soluplus<sup>®</sup> by Spray Drying Technique. *Chem. Pharm. Bull.* **2014**, *62*, 545–551. [[CrossRef](#)]
28. Schoubben, A.; Ricci, M.; Giovagnoli, S. Meeting the unmet: From traditional to cutting-edge techniques for poly lactide and poly lactide-co-glycolide microparticle manufacturing. *J. Pharm. Investig.* **2019**, *49*, 381–404. [[CrossRef](#)]
29. Cho, Y.; Ha, E.-S.; Baek, I.-H.; Kim, M.-S.; Cho, C.-W.; Hwang, S.-J. Enhanced Supersaturation and Oral Absorption of Sirolimus Using an Amorphous Solid Dispersion Based on Eudragit<sup>®</sup>. *E. Molecules* **2015**, *20*, 9496–9509. [[CrossRef](#)]
30. Das, S.; Ng, K.Y. Quantification of trans-resveratrol in rat plasma by a simple and sensitive high performance liquid chromatography method and its application in pre-clinical study. *J. Liq. Chromatogr. Relat. Technol.* **2011**, *34*, 1399–1414. [[CrossRef](#)]
31. Jansook, P.; Maw, P.D.; Soe, H.M.S.H.; Chuangchunsong, R.; Saiborisuth, K.; Payonitkarn, N.; Autthateinchai, R.; Pruksakorn, P. Development of amphotericin B nanosuspensions for fungal keratitis therapy: effect of self-assembled  $\gamma$ -cyclodextrin. *J. Pharm. Investig.* **2020**, *50*, 513–525. [[CrossRef](#)]
32. Luu, T.D.; Lee, B.-J.; Tran, P.H.L.; Tran, T.T.D. Modified sprouted rice for modulation of curcumin crystallinity and dissolution enhancement by solid dispersion. *J. Pharm. Investig.* **2019**, *49*, 127–134. [[CrossRef](#)]
33. Park, S.Y.; Kang, Z.; Thapa, P.; Jin, Y.S.; Park, J.W.; Lim, H.J.; Lee, J.Y.; Lee, S.-W.; Seo, M.-H.; Kim, M.-S.; et al. Development of sorafenib loaded nanoparticles to improve oral bioavailability using a quality by design approach. *Int. J. Pharm.* **2019**, *566*, 229–238. [[CrossRef](#)] [[PubMed](#)]
34. Vadlamudi, H.C.; Yalavarthi, P.R.; Nagaswaram, T.; Rasheed, A.; Peesa, J.P. In-vitro and pharmacodynamic characterization of solidified self microemulsified system of quetiapine fumarate. *J. Pharm. Investig.* **2019**, *49*, 161–172. [[CrossRef](#)]
35. Kim, D.-H.; Lee, S.-E.; Pyo, Y.-C.; Tran, P.; Park, J.-S. Solubility enhancement and application of cyclodextrins in local drug delivery. *J. Pharm. Investig.* **2020**, *50*, 17–27. [[CrossRef](#)]
36. Kim, M.-S.; Jin, S.-J.; Kim, J.-S.; Park, H.J.; Song, H.S.; Neubert, R.H.H.; Hwang, S.-J. Preparation, characterization and in vivo evaluation of amorphous atorvastatin calcium nanoparticles using supercritical antisolvent (SAS) process. *Eur. J. Pharm. Biopharm.* **2008**, *69*, 454–465. [[CrossRef](#)]
37. Baek, I.-H.; Kim, M.-S. Improved Supersaturation and Oral Absorption of Dutasteride by Amorphous Solid Dispersions. *Chem. Pharm. Bull.* **2012**, *60*, 1468–1473. [[CrossRef](#)]

38. Ha, E.-S.; Lee, S.-K.; Choi, D.H.; Jeong, S.H.; Hwang, S.-J.; Kim, M.-S. Application of diethylene glycol monoethyl ether in solubilization of poorly water-soluble drugs. *J. Pharm. Investig.* **2020**, *50*, 231–250. [[CrossRef](#)]
39. Won, D.-H.; Kim, M.-S.; Lee, S.; Park, J.-S.; Hwang, S.-J. Improved physicochemical characteristics of felodipine solid dispersion particles by supercritical anti-solvent precipitation process. *Int. J. Pharm.* **2005**, *301*, 199–208. [[CrossRef](#)]
40. Kojima, T.; Higashi, K.; Suzuki, T.; Tomono, K.; Moribe, K.; Yamamoto, K. Stabilization of a Supersaturated Solution of Mefenamic Acid from a Solid Dispersion with EUDRAGIT® EPO. *Pharm. Res.* **2012**, *29*, 2777–2791. [[CrossRef](#)]
41. Kim, M.-S. Influence of hydrophilic additives on the supersaturation and bioavailability of dutasteride-loaded hydroxypropyl- $\beta$ -cyclodextrin nanostructures. *Int. J. Nanomed.* **2013**, *8*, 2029–2039. [[CrossRef](#)] [[PubMed](#)]
42. Wegiel, L.A.; Mauer, L.J.; Edgar, K.J.; Taylor, L.S. Crystallization of Amorphous Solid Dispersions of Resveratrol during Preparation and Storage—Impact of Different Polymers. *J. Pharm. Sci.* **2013**, *102*, 171–184. [[CrossRef](#)] [[PubMed](#)]
43. Lin, X.; Su, L.; Li, N.; Hu, Y.; Tang, G.; Liu, L.; Li, H.; Yang, Z. Understanding the mechanism of dissolution enhancement for poorly water-soluble drugs by solid dispersions containing Eudragit® E PO. *J. Drug. Deliv. Sci. Tec.* **2018**, *48*, 328–337. [[CrossRef](#)]
44. Ramos, C. Development and validation of a headspace gas chromatographic method for determination of residual solvents in five drug substances. *Int. J. Pharm. Sci.* **2013**, *2*, 36–41.
45. Das, S.; Lin, H.S.; Ho, P.C.; Ng, K.Y. The impact of aqueous solubility and dose on the pharmacokinetic profiles of resveratrol. *Pharm Res.* **2008**, *25*, 2593–2600. [[CrossRef](#)] [[PubMed](#)]
46. Planas, J.M.; Alfaras, I.; Colom, H.; Juan, M.E. The bioavailability and distribution of trans-resveratrol are constrained by ABC transporters. *Arch. Biochem. Biophys.* **2012**, *527*, 67–73. [[CrossRef](#)] [[PubMed](#)]
47. Peñalva, R.; Morales, J.; González-Navarro, C.J.; Larrañeta, E.; Quincoces, G.; Peñuelas, I.; Irache, J.M. Increased oral bioavailability of resveratrol by its encapsulation in casein nanoparticles. *Int. J. Mol. Sci.* **2018**, *19*, 2816. [[CrossRef](#)]